Analysis of Distribution Static Compensator Control Strategies for Mitigating Voltage Dip Impact on Distribution Network

ABOYEDE ABAYOMI, AGHA F. NNACHI
Department of Electrical Engineering,
Tshwane University of Technology, eMalahleni,
SOUTH AFRICA

Abstract: - Voltage dip, over-voltage, load unbalanced, and current and voltage harmonics distortions are the key characteristics of poor power quality (PQ) issues on the power distribution network with a significant negative impact. The performance of a custom power device, distribution static compensator (D-STATCOM), in reducing current total harmonic distortion (THD) during the mitigation process of voltage dip with fault is investigated in this study. To control the load side voltage, the D-STATCOM utilizes a three-phase voltage source converter and is coupled at the point of common coupling (PCC). To mitigate voltage dip effects, this study implements and compares the effectiveness of the conventional PI controller with an intelligent optimization-based PI controller using the dynamic gravitational search algorithm (DGSA). The performance of these controllers is validated by the MATLAB/Simulink simulation results obtained. Analysis of the results demonstrates that D-STATCOM operates flawlessly with an intelligently optimized PI control strategy reducing the current THD from 11.68% to 3.74%.

Key-Words: - D-STATCOM, Dynamic Gravitational Search Algorithm, voltage dip correction, voltage regulation, grid optimization, stability.

Received: October 15, 2023. Revised: November 13, 2023. Accepted: December 6, 2023. Published: December 14, 2023.

1 Introduction

There has been an ongoing rise in global electricity usage with industrial and household loads consuming the largest portion of the globally generated power, [1]. Contemporary industrial processes heavily rely on large numbers of electronic devices, such as programmable logic controllers (PLCs) and adjustable-speed drives. Consequently, these industrial systems exhibit decreased tolerance to disruptions in power supply, such as brief interruptions, voltage fluctuations like dips and swells, flickers, and the presence of harmonics, [1]. Among these disturbances, voltage dips stand out as the most detrimental to industrial equipment, [2]. For instance, a mere 10% voltage drop lasting 100 milliseconds can significantly impact the operations of an electronic machine, [3]. Moreover, a voltage dip of 75% from the nominal voltage, enduring for less than 100 milliseconds, can incur substantial financial losses amounting to thousands of U.S. Dollars within the semiconductor industry, [4]. Nonlinear power electronic loads, such as converter-driven equipment, have distorted electrical power systems with undesired fluctuations in the voltage and current output, which leads to poor power quality (PQ), [2]. The opinions of utilities, equipment makers, and electric power end-users entirely differ when it comes to describing electric power quality. PQ is viewed by utilities in terms of system reliability. equipment manufacturers view PQ as a level that permits equipment to operate appropriately while the end-users view excellent PQ as the continued operation of equipment, activities, and enterprises. Any power issue that manifests as voltage, current, or frequency distortion that causes failures or malfunctions in customer equipment is referred to be a PQ issue, [3], [4], [5]. Due to their dispersed characteristics, renewable energy resources are widely installed to produce electricity on a modest scale. These power generators generally range in capacity from a few thousand kilowatts (kW) to several tens of megawatts (MW). The types of grid integration equipment utilized with photovoltaic (PV) and wind energies are power electronics converters and induction generators. Severe power quality issues including flicker, voltage dips, and other PQ issues may result from the integration of these devices into the distribution network, [6]. A few of the solutions presented by several studies that have investigated a range of power quality problems are highlighted below:

1.1 Voltage Regulation

Since conventional distribution networks were designed to handle load demand from the generation side, integrating distributed generation (DG) into existing power networks potentially results in several PQ issues. Being that these network designers anticipated unidirectional power flow, however, with DG penetration of the distribution network, power flow becomes bidirectional because the DG produces additional power that is fed back to the generation side. The distribution system's operation, voltage regulation, and system protection are all significantly affected by bidirectional power flow. As a result, two different approaches to controlling voltage in the distribution networks have been studied and presented. These strategies are classified into two categories: conventional and contemporary, [7]. The conventional method involves active network management. Setting up appropriate management policies that the distribution network operators (DNO) could implement including real-time monitoring, communication, and network control. Step voltage regulators, also known as Static Voltage Regulators (SVR), On-Load Tap Changer (OLTC), and distribution static compensators (D-STATCOM) are the common equipment used in the conventional method for voltage regulation, [8]. Another method to maintain the distribution network voltage at desirable levels is intelligent distributed control, which involves machine learning techniques, [9], [10], [11]. A three-phase D-STATCOM with three-phase unbalanced grid current compensation, total harmonic distortion (THD) reduction of the grid current, and power factor (PF) correction was suggested in, [12] as a way to enhance power quality. A new online trained wavelet Takagi-Sugeno-Kang fuzzy neural network (WTSKFNN) controller was utilized in place of the conventional proportional-integral (PI) controller to improve the D-STATCOM performance and transient responses of the grid currents and DC-link voltage control. The experimental findings confirmed the viability and efficiency of intelligently controlled D-STATCOM for improving power quality and controlling the DC-link voltage under load variation. The Lyapunov stability theory was proposed in, [13], to demonstrate the stability of the enhanced first-order linear active disturbance rejection controller (LADRC), which corrects the error of the total disturbance and improves track anti-interference performance. To enhance the system's anti-interference capabilities and the linear extended state observer's (LESO) ability to perceive interference in the presence of high-frequency noise, the output of the complete interference channel is rectified. According to the experimental findings, the enhanced LADRC controller has better tracking and anti-interference performance than the proportional-integral (PI) controller.

1.2 Voltage Dip

Research studies have established voltage dip as one of the most frequent occurrences in power systems. Industrial machines are becoming increasingly automated. The fundamental equipment – microelectronics, power electronics, and high-tech precision tools become susceptible to voltage dip, [14], [15]. Therefore, reducing the number of voltage dips and their impact needs coordinated efforts from the power supply side, client side, and equipment manufacturer side, [16], [17]. Consequently, measures to mitigate power supply side voltage dips include prevention and control, which limit the frequency and duration of short-circuit faults as well as the damage caused by voltage dips. Installation of custom power devices (CPD) such as distribution static compensators (D-STATCOM), active voltage conditioners (AVC), and dynamic voltage restorers (DVR) on the client side mitigates voltage dip at the point of common coupling (PCC). In addition, the CPD also controls three-phase unbalance, compensates reactive power, and generally enhances power quality. The introduction of D-STATCOM, a cost-effective and viable solution to enhance the performance of the distribution network has been studied in, [13]. D-STATCOM, a dynamic reactive power compensation device, mitigates voltage fluctuations and power loss, increases the system power factor, and efficiently stabilizes the voltage. It is a crucial device for enhancing power supply reliability and power quality regulation, [17]. The tracking control of the compensating current is connected to reactive current compensation, which is the main technological feature of the D-STATCOM compensatory current. Hence, research on the D-STATCOM AC side current control method has gotten a lot of attention and the implementation of D-STATCOM for improved power quality during voltage dip on the client side is the emphasis of this study. The conventional linear control strategy, which primarily linearizes the system of the nonlinear mathematical model of D-STATCOM, is the major technique used in current loop control. The study in, [18], decouples the system into the dq0 synchronous coordinate system using a PI controller since the control structure of the PI controller is uncomplicated, however, its performance drops if the actual operating conditions are different from the assumptions, particularly when there are significant short-circuit faults or sharp disturbances from heavy load changes. As a result, other intelligent control optimization strategies have been developed in the context of the limitations of PI controllers. A Dynamic Gravitational Search Algorithm (DGSA) controlled D-STATCOM was implemented in this study to mitigate the impact of voltage dips and smooth the grid voltage profile. The benefit of this control strategy for reactive power compensation, voltage dip mitigation, and current total harmonic distortion (THD) reduction is demonstrated by simulation results and compared to the results of the conventional PI controller.

2 The D-STATCOM Circuit Design

To increase the dynamic performance of the power distribution network when the grid voltage dips, this study advances the idea of intelligently regulating a D-STATCOM device for an efficient distribution network. Figure 1 depicts the equivalent circuit of a D-STATCOM, which is designed with a coupling transformer's reactance, linked with the AC system, a DC bus, and a power inverter built using power electronic components.

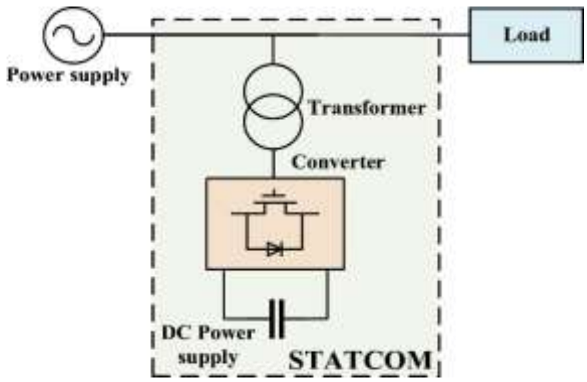

Fig. 1: D-STATCOM equivalent circuit.

The control strategy for power transfer between the converter and the distribution network, which also depends on the converter's alternative output voltage, is subject to the basic operating principle of D-STATCOM. The following statement summarizes the operating principle:

- If the distribution network voltage amplitude is lower than the D-STATCOM output voltage, the D-STATCOM injects reactive power then the current flows through the reactance to the network.
- If the amplitude of the D-STATCOM output voltage is lower than that of the network, the D-STATCOM absorbs reactive power from the network for current to flow to the network.
- If the converter's output voltage equals that of the network, the D-STATCOM remains at an equilibrium state and the reactive power exchange value will be zero.

The D-STATCOM main circuit depicted in Figure 1, has the following structural components: the voltage support capacitor, which is utilized to support the device's voltage; the voltage source converter (VSC) is made up of power electronic switching components controlled by space vector pulse width modulation (SVPWM). The filter is used to remove high-order harmonics from the inverter output voltage, converting the capacitor's DC voltage into an AC voltage with a specific amplitude and frequency that is approximate to a sine wave. The grid-connected inverter's ability to provide effective control has a significant impact on the output power quality. The overall control structure of the voltage-type D-STATCOM is depicted in Figure 2, where the three-phase grid voltage is denoted with u_{sa}, u_{sb}, and u_{sc}; i_{ca}, i_{cb}, and i_{cc} for the compensator's output current; u_{ca}, u_{cb}, and u_{cc} for the D-STATCOM's output voltage; u_{dc} for the voltage of the DC side capacitor; and R, L for the filter's equivalent resistance and inductance is also connected with the D-STATCOM in parallel to smoothen the compensation currents.

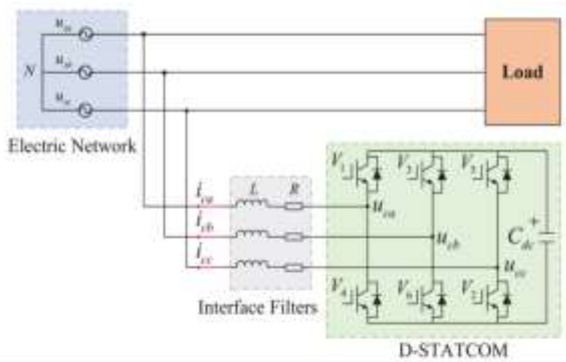

Fig. 2: D-STATCOM control structure.

3 The D-STATCOM Control Algorithm

The control strategy used to generate the VSC switch signals affects the performance of D-STATCOM at the PCC. The fundamental objective of the D-STATCOM control model is to reduce the impact of voltage dip and mitigate THD using two different control methods. The D-STATCOM operation is activated by obtaining the source voltage amplitude, reference current, and error signal from the actual current and the generated current. The device VSC switching is controlled by the derived error to manage the D-STATCOM bi-directional flow of active power. The MATLAB/Simulink program was used to simulate the proposed DGSA methodology, and the results were contrasted to those of a conventional PI controller.

3.1 PI Controll]er

PI controllers have been utilized to enhance steady-state and transient performance as well as for the elimination of sudden disturbances brought on by operational events, [19], [20]. The controller includes both proportionate and integral actions. By utilizing the proportion of system error to regulate the system, the proportional controller reduces system error. It however introduces into the system an offset error. The output of the integral controller is proportional to how long an error has been present in the system. The offset introduced by the proportional control is removed by the integral action. PID tuning with actuator restriction has been used in this study to optimize the K_P and K_I tuning parameters for the PI controller. Figure 3 illustrates the block diagram used to determine the PI controller parameters.

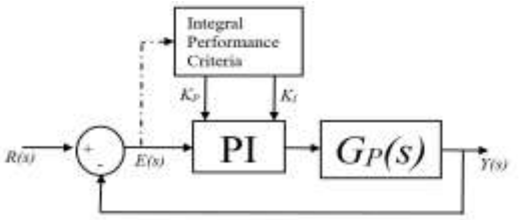

Fig. 3: Simulink model of the system control.

Where $R_{(s)}$, $E_{(s)}$ and $Y_{(s)}$ denote the input signal, the output signal and the error respectively. Using a PI controller, the tuning parameters are controlled to ensure that the D-STATCOM DC capacitor voltage does not deviate from the reference value. The control output of the PI controller is given by Equations (1) and (2). The integral performance criteria have been defined by using the integral squared error (ISE) expressed in Equation (3) to choose the appropriate controller parameters based on the error in the control system.

$$e(t) = r(t) - y(t)$$
$$u(t) = K_P e(t) + \frac{K_P}{K_I}\int_0^t e(t)dt \quad (1)$$

$$P = K_P(v_{dc\_ref} - v_{dc}) + K_I \int (v_{dc\_ref} - v_{dc})dt \quad (2)$$

$$ISE = \int_0^\infty e^2(t) \times dt \quad (3)$$

The optimized Simulink block diagram in Figure 3 is run to determine the controller parameters. Table 1 presents the PI controller parameters for the designed system using integral performance criteria.

Table 1. PI Controller Gain

Parameter	K_P	K_I
Gain with actuator	3.675	-0.4672

The error in the dc link voltage serves as the PI controller's input, and its output is the amount of power exchanged by the D-STATCOM at the PCC. The value of the power is influenced by K_P, K_I, and dc-link voltage error values. Therefore, the gains must be correctly tuned. However, it is challenging to adjust the controller's gains because of the system's intrinsic nonlinearity and complexity. Usually, it involves a lot of trial and error. Therefore, the DGSA-optimized PI controller has been used in place of the conventional PI controller because it is simpler, easier to implement, and more resilient to system uncertainties and disturbances.

3.2 DGSA-based PI Controller

An intelligent algorithm, the dynamic gravitational search algorithm (DGSA) based on Newtonian laws and mass interactions is implemented to optimally tune the D-STATCOM PI controller due to its rapid convergence property of errors in finite time. The population in this algorithm is referred to as masses, and performance is assessed by the masses' position. Position, inertial mass, active gravitational mass, and passive gravitational mass are the four characteristics of each mass. While the mass's gravitational and inertial masses related to the fitness function, the mass's position represented a solution. Newtonian laws state that gravity will cause all of these particulars to gravitate toward one another. Due to this force, heavier weight masses which are equivalent to excellent solutions, move more slowly than lighter masses, which are equivalent to bad solutions. The global solution and the problem's overall fitness at the final recorded iterations are determined by the finest fitness and position of the relevant agent within the search space. The algorithm's exploitation stage in the system is modeled and depicted in Figure 4.

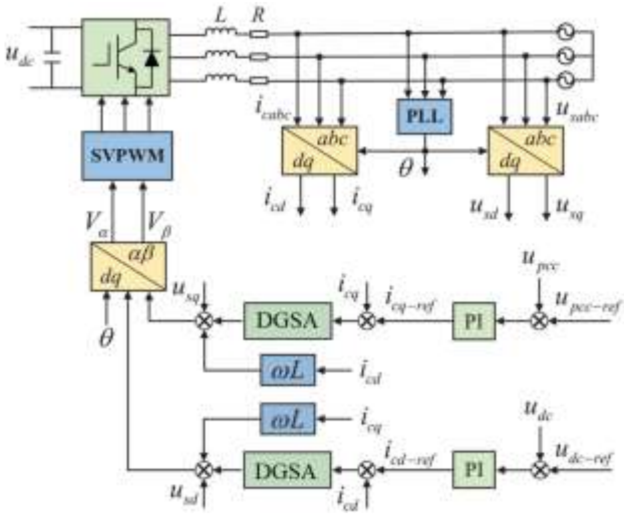

Fig. 4: D-STATCOM control structure with DGSA.

In a system comprising n masses, Equation (4) provides the position W_i for the i-th mass.

$$W_i = \left(W_i^1, \dots W_i^d, \dots W_i^n\right) \, for \; i = 1,2 \dots n \qquad (4)$$

Where W_i^d is the ith mass position in the dth dimension. At a specific time t, Equation (5) describes the force exerted by mass j on mass i.

$$G_{i,j}^d(t) = F(t) \, \frac{C_{pi}(t) \times C_{ai}(t)}{D_{i,j}(t) + \varepsilon} \left[W_j^d(t) - W_i^d(t)\right] \qquad (5)$$

In Equation (8), $C_{pi}(t), C_{ai}(t) \; and \; D_{i,j}(t)$ correspond to the active gravitational mass associated with agent j with gravitational constant at time t, passive gravitational mass is linked to agent i and ε is the Euclidian distance between two mass i and j respectively.

Within a d-dimensional space, the cumulative force acting on mass i can be determined with Equation (6).

$$G_i^d(t) = \sum_{j=1, j\neq 1}^{n} rand_j G_{i,j}^d(t) \qquad (6)$$

Therefore, the acceleration of mass i at time t within the dth dimension, as defined by the principles of motion, is represented in Equation (7).

$$a_i^d(t) = \frac{G_i^d(t)}{D_{i,i}(t)} \qquad (7)$$

where Dii represents the inertia of the ith mass. The modification of a mass's velocity depends on both its current velocity and acceleration. Equations (8) and (9) outline the velocity and position of the mass.

$$v_i^d(t+1) = rand_i v_i^d(t) + a_i^d(t) \qquad (8)$$

$$W_i^d(t+1) = W_i^d(t) + v_i^d(t+1) \qquad (9)$$

To commence, a randomized attribute is employed in the search process, where a random number is utilized to calculate the gravitational constant, thus regulating the accuracy of the DGSA. The evaluation of inertia masses and the gravitational search relies on the fitness function, which is associated with the more heavier masses in Equations (10) and (11).

$$m_i(t) = \frac{stable_i(t) - unstable_i(t)}{best\;(t) - worst\;(t)} \qquad (8)$$

$$M_i(t) = \frac{m_i\;(t)}{\sum_{j=1}^{n} m_j\;(t)} \qquad (9)$$

Where stable i (t) denote ith mass fitness value at time t and best (t) for a minimization cost defined by Equation (10).

$$\begin{gathered} Best\;(t) = Min\;\; stable_j(t) \\ Worst\;(t) = Max\;\; stable_j(t) \end{gathered} \qquad (10)$$

Equations (11) and (12) define the algorithmic processes to optimize the gain parameter of the PI controller. While Equation (13) calculates the voltage error.'

$$K_P(\delta) = K_P(\delta - 1) + \Delta K_P(\delta - 1) \qquad (11)$$

$$K_I(\delta) = K_I(\delta - 1) + \Delta K_I(\delta - 1) \qquad (12)$$

$$V_{pcc}(\delta) = V^*{}_{dc}(\delta) - V_{dc}(\delta) \qquad (13)$$

When carefully chosen, an objective function is a crucial component of any optimization process and enhances system performance while fulfilling the requirements of the control design. Applying D-STATCOM to the grid-tied PV system is intended to reduce voltage deviation by adjusting the error input from the current controllers to zero steady-state. The D-STATCOM may not adjust for the power quality concerns or may function at a lesser efficiency if the dc-link voltage is not kept at its reference value or the PI controller gain parameters are not properly calibrated. The Proportional (P) phase of the PI controller gives a quick response, while the Integral (I) phase assures there is no steady-state inaccuracy. Together with each other, these two phases work to regulate the dc-link voltage. The optimization objective function was the Integral Square Error (ISE) performance index 'J,' denoted in Equation (13).

$$J = ISE = \int_{0}^{Ts} e_d^2 + e_q^2 \tag{13}$$

$$Error(e_r) = (i_d - i_{dref})^2 + (i_q - i_{qref})^2$$

A minimizing cost function was selected for better compensation and to reduce the input error. The optimization's objective was to track the best values for the parameters that were to be optimized so that the error input of the D-STATCOM current controllers could be maintained at zero steady-state. The maximum sensitivity function that measures the robustness of a PI controller tuning algorithm is defined by Equation (14).

$$M_S = \max|S(j\omega)| \tag{14}$$

where: M_S is the maximum sensitivity function, max|S(jω)| is the impact of feedback on the output.

The value of M_S ranges from 1.1 to 2 and provides reasonable robustness of the closed-loop when max|S(jω)| < 1, the disturbances are mitigated and amplified when max|S(jω)| > 1. The robustness of the closed-loop increases with the decrease in M_S.

4 Simulation Result and Discussion

The simulation of the proposed DGSA-controlled PI controller methodology has been carried out by using the MATLAB/Simulink software and compared the results with a conventional regulated PI controller. A voltage dip fault in the electrical distribution network as shown in Figure 5 was used to simulate a capacitive operation mode in the electrical distribution network to evaluate the dynamic behaviour of the system analyzed with these two types of controllers. Keeping the PCC reference voltage constant at 1 pu, a voltage dip is introduced to the PCC at time t = 0.05 second. Figure 5 presents the simulation results for the voltage at PCC without D-STATCOM compensation, and Figure 6 illustrates the voltage at PCC with the control configuration using a conventional PI D-STATCOM compensation.

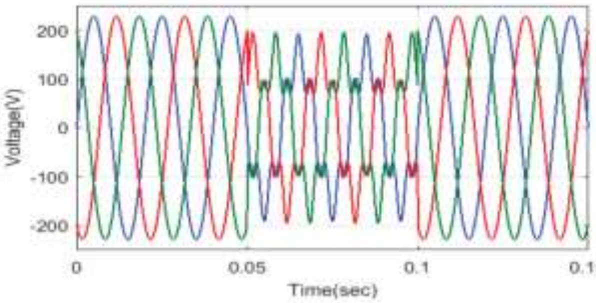

Fig. 5: Voltage at PCC without compensation from D-STATCOM.

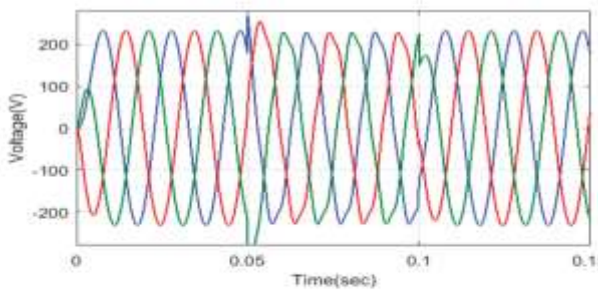

Fig. 6: Voltage at PCC with D-STATCOM compensation.

Figure 7 depicts the spontaneous damping of the induced voltage faults by the D-STAMCOM. Figure 8 presents in comparison to a control loop based on the conventional PI controller, the voltage dip induced at the instant t=0.5 second is automatically compensated by the DGSA-controlled D-STATCOM with less oscillation and minimized error. The differences in the thickness of the voltage response achieved by the conventional PI controller and that obtained by the proposed DGSA controller indicate the better performance of the proposed method. Since the voltage feeds the current loop, which is characterized as the inner loop, these oscillations affect the responses of the current. The proposed controller compensates for the high-frequency oscillations that make up the signal thickness.

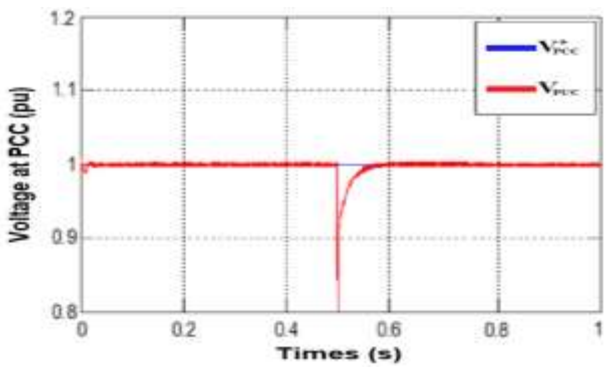

Fig. 7: Voltage profile at PCC with conventional PI D-STATCOM controller.

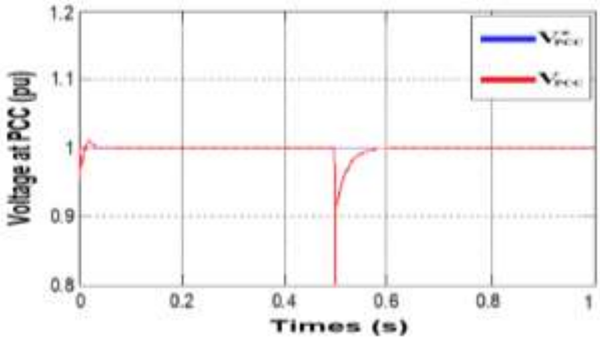

Fig. 8: Voltage at PCC with D-STATCOM compensation.

Figure 9a and Figure 9b indicate that the reactive current is positive by 0.5 to 1 second, indicating that the D-STATCOM is operating in capacitive mode (producing reactive power to counteract the voltage dip) at the PCC. In addition, compared to a D-STATCOM running through a conventional PI controller, the static error in the D-STATCOM's response to the DGSA is decreased.

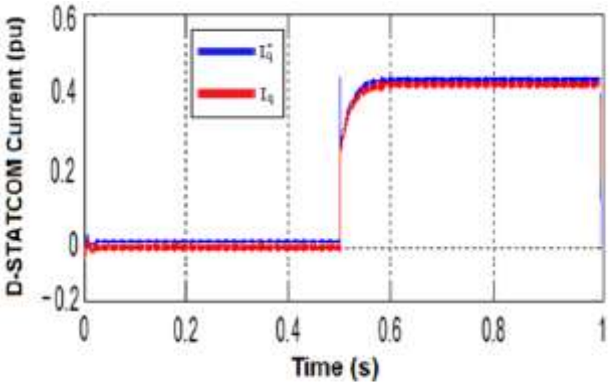

Fig. 9a: D-STATCOM conventional PI controller dynamic reactive currents

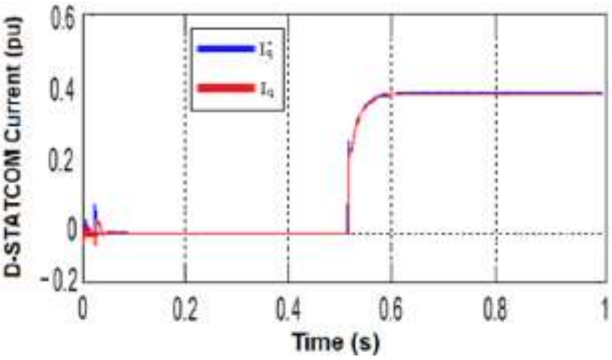

Fig. 9b: D-STATCOM with a DGSA controller dynamic reactive currents

The dynamic responses of the D-STATCOM's active and reactive powers are depicted in Figure 10. The figures show how the D-STATCOM operates in an inductive mode for 0.5 to 1 second, supplying the reactive power required to keep the voltage steady in a power distribution network.

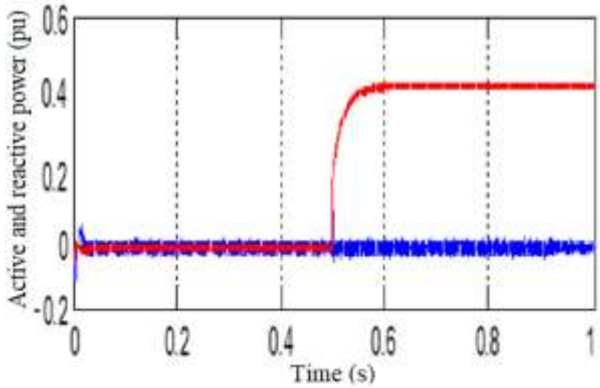

Fig. 10: D-STATCOM active and reactive powers dynamic response.

In addition, by comparing the reactive powers provided using the proposed control method in Figure 11, an error reduction is achieved with less oscillation compared to the system using the conventional PI controller.

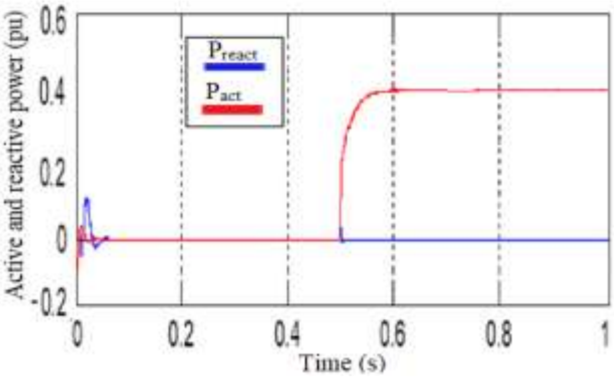

Fig. 11: DGSA controlled D-STATCOM active and reactive powers dynamic response.

Table 2 presents the spectrum analysis of current harmonics injected by the D-STATCOM. It is noted that with the use of the DGSA-controlled method, the harmonics in these injected currents are reduced compared to the conventional PI controller-based D-STATCOM. The current total harmonic distortion (THD) for the D-STATCOM with the conventional PI controller is 11.68%, while the THD spectrum analysis for DGSA-controlled D-STATCOM is 3.74%. Hence, the proposed optimized controller demonstrates better performance in terms of current harmonics reduction.

Table 2. Current Harmonics Analysis

Description	Result
Conventional PI controller	11.68%
DGSA-controlled device	3.74%

5 Conclusion

The simulation of the proposed Dynamic Gravitational Search Algorithm (DGSA) controlled D-STATCOM strategy was implemented in this study to mitigate the impact of voltage dips and smooth the grid voltage profile. The benefit of this control strategy for reactive power compensation, voltage dip mitigation, and current total harmonic distortion (THD) reduction is demonstrated by the simulation results and compared to the results of the conventional PI controller. The simulation results show that the proposed control method for D-STATCOM not only achieves sinusoidal and symmetrical grid current with fewer harmonics, in addition efficiently eliminates the oscillation produced in active and reactive power. The DGSA-optimized PI control strategy reduced the current THD from 11.68% to 3.74% below the maximum standard limit of 5% helps mitigate the effect of voltage dip and improves the overall performance of the distribution network.

References:

[1] Lumbreras, D., Gálvez, E., Collado, A. and Zaragoza, J.. Trends in power quality, harmonic mitigation and standards for light and heavy industries: A review. *Energies*, vol. 13, no. 21, 2020, pp. 1 – 24.

[2] Montoya, F.G., Baños, R., Alcayde, A., Montoya, M.G. and Manzano-Agugliaro, F. Power quality: Scientific collaboration networks and research trends. *Energies*, vol. 11, no. 8, 2018, pp. 1 –26.

[3] Bollen, M.H. What is power quality? *Electric power systems research*, vol. 66, no. 1, 2003, pp. 5-14.

[4] Bollen, M.H., Styvaktakis, E. and Gu, I.Y.H. Categorization and analysis of power system transients. *IEEE Transactions on Power Delivery*, vol. 20, no. 3, 2005, pp. 2298-2306.

[5] Bajaj, M. and Singh, A.K. Grid integrated renewable DG systems: A review of power quality challenges and state-of-the-art mitigation techniques. *International Journal of Energy Research*, vol. 44, no. 1, 2020, pp.26-69.

[6] Kumar, V., Pandey, A.S. and Sinha, S.K. Grid integration and power quality issues of wind and solar energy system: A review. In proceeding of *IEEE International conference on emerging trends in electrical electronics & sustainable energy systems*, 2016, pp. 71-80.

[7] Chaudhary, P. and Rizwan, M. Voltage regulation mitigation techniques in distribution system with high PV penetration: A review. *Renewable and Sustainable Energy Reviews*, vol. 82, 2018, pp. 3279-3287.

[8] Razavi, S.E., Rahimi, E., Javadi, M.S., Nezhad, A.E., Lotfi, M., Shafie-khah, M. and Catalão, J.P. Impact of distributed generation on protection and voltage regulation of distribution systems: A review. *Renewable and Sustainable Energy Reviews*, vol. 105, 2019, pp.157-167.

[9] Fetouh, T. and Elsayed, A.M. Optimal control and operation of fully automated distribution networks using improved tunicate swarm intelligent algorithm. *IEEE Access*, vol. 8, 2020, pp.129689-129708.

[10] Shaheen, A.M., Elattar, E.E., El-Sehiemy, R.A. and Elsayed, A.M. An improved sunflower optimization algorithm-based Monte Carlo simulation for efficiency improvement of radial distribution systems considering wind power uncertainty. *IEEE Access*, vol. 9, 2020, pp. 2332-2344.

[11] Wang, B., Zhu, H., Xu, H., Bao, Y. and Di, H. Distribution network reconfiguration based on NoisyNet deep Q-learning network. *IEEE Access*, vol. 9, 2021, pp. 90358-90365.

[12] Chen, J.H, Tan, K. and Lee, Y. "Intelligent Controlled DSTATCOM for Power Quality Enhancement." *Energies*, vol. 15, no. 11, 2022, pp. 1-19.

[13] Zhou, X., Zhong, W., Ma, Y., Guo, K., Yin, J., Wei, C. "Control strategy research of D-STATCOM using active disturbance rejection control based on total disturbance error compensation." *IEEE Access*, vol. 9, 2021, pp. 50138–50150.

[14] Rauf, A.M. and Khadkikar, V. "An enhanced voltage sag compensation scheme for dynamic voltage restorer." *IEEE Transactions on Industrial Electronics*, vol. 62, no. 5, pp. 2683-2692, 2014

[15] Molla, E.M. and Kuo, C.C. Voltage sag enhancement of grid-connected hybrid PV-wind power system using battery and SMES based dynamic voltage restorer. *IEEE Access*, vol. 8, 2020, pp. 130003-130013.

[16] Tang, L., Han, Y., Yang, P., Wang, C., and Zalhaf, A.S. A review of voltage sag control measures and equipment in power systems. *Energy Reports*, vol. 8, 2022, pp. 207-216.

[17] Adebiyi, A.A. and Akindeji, K.T. "Investigating the effect of static synchronous compensator (STATCOM) for voltage enhancement and transmission losses mitigation." Proceedings of the *IEEE PES-IAS PowerAfrica Conference,* 2017, pp. 462-467.

[18] Wang, P., Wang, Y., Jiang, N. and Gu, W. "A comprehensive improved coordinated control strategy for a STATCOM integrated HVDC system with enhanced steady/transient state behaviors", *International Journal of Electrical Power Energy System*, vol. 121, 202, pp. 1-19.

[19] Meena, P., Dua, P., Maji, N. and Arora, A., "Control of DSTATCOM in distribution systems by artificial intelligence based controller." In Proceeding of the *IEEE International Conference on Distributed Computing and Electrical Circuits and Electronics (ICDCECE)*, 2022, pp. 1.

[20] Adebiyi, A.A., Lazarus, I.J., Saha, A.K. and Ojo, E.E., "Performance analysis of the grid-tied photovoltaic system under varying weather condition and load." *International Journal of Electrical and Computer Engineering*, vol. 11, no. 1, 2021, pp. 94-106.

Contribution of Individual Authors to the Creation of a Scientific Article (Ghostwriting Policy)

The authors made equal and substantial contributions to this research, participating in all stages, from defining the research context to the conclusion.

Sources of Funding for Research Presented in a Scientific Article or Scientific Article Itself

I want to use this [opportunity to appreciate Tshwane University of Technology for the success of this research work.

Conflict of Interest

The authors have no conflicts of interest to declare that are relevant to the content of this article.